Railton, CJ., Paul, DL., & Pothecary, NM. (1994). Calculation of the dispersive characteristics of open dielectric structures by the finite-difference time-domain method. *IEEE Transactions on Microwave Theory and Techniques*, *42*(7), 1207 - 1212. https://doi.org/10.1109/22.299758

# Calculation of the Dispersive Characteristics of Open Dielectric Structures by the Finite-Difference Time-Domain Method

Dominique-Lynda Paul, Nick M. Pothecary, and Chris J. Railton

*Abstract*— **An enhanced three-dimensional Finite-Difference Time-Domain (FDTD) technique is applied to the characterization of the fundamental and higher order modes of single and coupled image guide structures. The basic FDTD algorithm is modified to include multidimensional changes of permittivity and an irregular mesh is used for computational efficiency. In this paper FDTD calculations are compared with experimental and theoretical results found in the literature and good agreement is found.**

## I. Introduction

In the last two decades, open dielectric structures, namely the image guide and its derivatives, have been extensively studied for application at millimeter and submillimeter wave frequencies [1]–[3] and many numerical or quasi-analytical techniques have been proposed to solve the eigenvalue problem for such guides. Among them, the Effective Dielectric Constant (EDC) method is the most widely used analysis technique for its simplicity and its versatility, however although its accuracy is satisfactory for most engineering applications, it is only an approximate method.

The FDTD technique has the advantage of being both rigorous and very versatile. Currently, it is becoming increasingly popular for analyzing numerous microwave applications and it has shown great success in the modeling of microstrip planar circuits [4]–[6]. In its two-dimensional version and making use of a regular mesh, the technique has been applied to guided-wave structures in the optical frequency range [7] and to boxed image guides [8] and boxed coupled dielectric guides [9] in the microwave range. Making use of a graded mesh, the 2-D version has recently proved to be an interesting method for the modeling of various open dielectric structures [10]. The two-dimensional version is certainly well suited to the analysis of uniform waveguiding structures, however, a full three-dimensional approach is needed to model discontinuities. In addition, the 2-D approach may become cumbersome when analyzing lossy structures due to the need to search for solutions in the complex plane. In this contribution, we shed light on the extra complications linked to the application of the 3-D FDTD technique. We use a modified FDTD algorithm and a nonuniform mesh to show that a full-wave 3-D FDTD technique can be applied to the characterization of open dielectric structures. Having described the main steps of the theoretical approach (including enhancements to the basic algorithm, excitation of a particular mode, etc.), results will be presented for single and coupled image guides (see insets of Figs. 3 and 4). Comparison with other available techniques shows the validity of the method.

Manuscript received February 3, 1993; revised September 14, 1993.

The authors are with the Centre for Communications Research, Faculty of Engineering, University of Bristol, Bristol BS8 1TR, U.K.

IEEE Log Number 9402374.

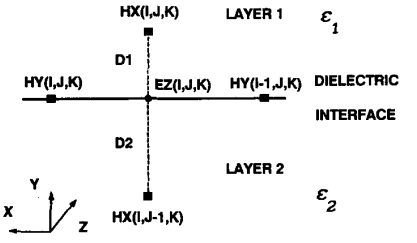


Fig. 1. Illustration of a change of permittivity in the $y$ direction.

## II. Theory

### A. Modification of the FDTD Algorithm for Dielectric Boundaries

The basic 3-D FDTD method has been presented in various publications [4]–[6] and need not be detailed here. However, in order to model the image guide, it is necessary to account for changes of permittivity in two dimensions. As shown in [11], if the mesh is regular (i.e., a uniform space-step between nodes) it is possible to use the average value of the dielectric constants at a dielectric boundary, but for the more general case of a nonuniform grid and two-dimensional permittivity changes a more rigorous approach must be used.

*1) One-Dimensional Dielectric Boundaries:* Consider the calculation of the $E_z$ field component when there is a dielectric change in the $y$ direction. Fig. 1 shows the spatial arrangement of the fields used in the calculation. The problem is that the field gradients in individual dielectric layers are unknown quantities. The field is available only at discrete points (nodes) and normal FDTD calculation assumes a linear change between such points. However if dielectric boundaries are present then the electric field component normal to the dielectric boundary will exhibit sharp changes and hence will no longer be linear. To overcome this difficulty it is necessary to find an expression for the field gradients in individual dielectric layers.

For two adjacent layers 1 and 2 the field gradient $\partial H_y/\partial x$ is assumed constant along the boundary and the tangential electric field is continuous across the boundary. The general form of Maxwell's equation for the $\boldsymbol{E_z}$ field component can be written as

$$\frac{\partial E_z}{\partial t} = \frac{1}{\epsilon}\left(\frac{\partial H_y}{\partial x} - \frac{\partial H_x}{\partial y}\right) - \frac{\sigma}{\epsilon}E_z \tag{1}$$

but from [11] (1) becomes

$$\frac{\partial E_z}{\partial t} = \frac{1}{\epsilon_1}\left(\frac{\partial H_y}{\partial x} - \left.\frac{\partial H_x}{\partial y}\right|_1\right) - \frac{\sigma_1}{\epsilon_1}E_z \tag{2}$$

where

$$\left.\frac{\partial H_x}{\partial y}\right|_1 = \frac{\delta H_x - \sum_{i=1}^{2} d_i\left(1-\frac{\epsilon_i}{\epsilon_1}\right)\frac{\partial H_y}{\partial x} + \sum_{i=1}^{2} d_i\left(\sigma_i - \frac{\sigma_i}{\epsilon_1}\right)E_z}{\sum_{i=1}^{2} d_i\frac{\epsilon_i}{\epsilon_1}} \tag{3}$$

and $\delta H_x$ represents the actual difference in field values between two nodes.

$$\delta H_x = \sum_{i=1}^{2}\left.\frac{\partial H_x}{\partial y}\right|_i d_i. \tag{4}$$

A set of coefficients

$$P_1^y = \sum_{i=1}^{2} d_i\left(1-\frac{\epsilon_i}{\epsilon_1}\right)$$

$$p_2^y = \sum_{i=1}^{2} d_i\frac{\epsilon_i}{\epsilon_1}$$

$$P_3^y = \sum_{i=1}^{2} d_i\left(\sigma_i - \frac{\epsilon_i}{\epsilon_1}\sigma_1\right) \tag{5}$$

can be used to simplify (3) to give

$$\left.\frac{\partial H_x}{\partial y}\right|_1 = \frac{\delta H_x - P_1^y\frac{\partial H_y}{\partial x} + P_3^y E_z}{P_2^y} \tag{6}$$

which represents the unknown field gradient in dielectric layer 1 in terms of known quantities. Equation (6) can now be substituted into (2) to give an expression for the electric field $\boldsymbol{E_z}$.

*2) Extension to Two-Dimensional Dielectric Boundaries:* Similarly if the dielectric change occurs in the $x$ direction

$$\left.\frac{\partial H_y}{\partial x}\right|_1 = \frac{\delta H_y - P_1^x\frac{\partial H_x}{\partial y} - P_3^x E_z}{P_2^x}. \tag{7}$$

Equations (6) and (7) can now be combined by substituting (6) into (7) to give

$$\left.\frac{\partial H_y}{\partial x}\right|_1 = \frac{P_2^y\delta H_y - P_1^x\delta H_x - P_1^x P_3^y E_z - P_2^y P_3^x E_z}{P_2^x P_2^y - P_1^x P_1^y} \tag{8}$$

and similarly, substituting (7) into (6) gives

$$\left.\frac{\partial H_x}{\partial y}\right|_1 = \frac{P_2^x\delta H_x - P_1^y\delta H_y + P_1^y P_3^x E_z + P_2^x P_3^y E_z}{P_2^x P_2^y - P_1^x P_1^y}. \tag{9}$$

Now that we have expressions for the field gradients in a single dielectric layer the final step is substitution of these equations into (2) to give (after discretization):

$$\boldsymbol{E}_z^{n+1} = \frac{1-\frac{\sigma_1\delta t}{2\epsilon_0\epsilon_1}}{1+\frac{\sigma_1\delta t}{2\epsilon_0\epsilon_1}}\boldsymbol{E}_z^n + \frac{\delta t}{\epsilon_0\epsilon_1\left(1+\frac{\sigma_1\delta t}{2\epsilon_0\epsilon_1}\right)} \cdot \left(\frac{\delta H_y(P_1^y+P_2^y) - \delta H_x(P_1^x+P_2^x) - KE_z^n}{P_2^x P_2^y - P_1^x P_1^y}\right) \tag{10}$$

where

$$K = P_1^x P_3^y + P_2^y P_3^x + P_1^y P_3^x + P_2^x P_3^y$$

Equation (10) is used to calculate the $\boldsymbol{E_z}$ field component at a dielectric boundary instead of the normal finite-difference expression, valid for a uniform medium of permittivity $\epsilon_1$:

$$\boldsymbol{E}_z^{n+1} = \frac{1-\frac{\sigma_1\delta t}{2\epsilon_0\epsilon_1}}{1+\frac{\sigma_1\delta t}{2\epsilon_0\epsilon_1}}\boldsymbol{E}_z^n + \frac{\delta t}{\epsilon_0\epsilon_1\left(1+\frac{\sigma_1\delta t}{2\epsilon_0\epsilon_1}\right)}\left[\left(\frac{\delta H_y}{\delta x}\right) - \left(\frac{\delta H_x}{\delta y}\right)\right]. \tag{11}$$

The coefficients of (10) can be calculated before the main iteration loop and they take account of a nonuniform grid and any dielectric losses. Similar expressions can be derived for the $\boldsymbol{E_x}$ and $\boldsymbol{E_y}$ field components.

### *B. Boundary Conditions*

A perfect electric wall is used as a ground plane but in order to simulate an open structure, Absorbing Boundary Conditions (ABC's) must be employed to limit the domain. Most available ABC's are designed to absorb traveling waves impinging at normal incidence and will be efficient in such cases. However, in the cross-sectional plane of the image guide the wave arrives with angles other than normal incidence. This is most noticeable on the upper boundary as the wave impinges with a grazing angle if the limit of the computational domain is placed close to the substrate. Hence to avoid problems caused by the ABC's being too close to the structure they must be placed sufficiently far away from the dielectric core. For the image guide, the ABC's must be put at a distance of approximately 5 times the substrate half-width, $a$, and 7 times the substrate height, $b$, with the additional constraint that the space step close to the boundary is around $\lambda/10$ for Mur's first-order ABC [12] or $\lambda/20$ for Mur's second-order ABC [12], $\lambda$ being the wavelength corresponding to the cutoff frequency of the mode.

For these reasons, although other boundary conditions exist which have theoretically better performance for plane wave incidence, Mur's first-order ABC's are most appropriate to this application and are employed here.

### C. The Mesh

If the dispersion characteristics of the guide are to be obtained over a wide frequency range the size and density of the mesh are subject to two requirements:

- as pointed out in the preceding section, the boundaries must be placed sufficiently far away in the cross-sectional plane to achieve accuracy around the cutoff frequency.
- at high frequencies, the energy is confined to the dielectric and since the maximum region size in the structure is dependent upon the highest frequency of interest, this places constraints on the mesh size. As will be illustrated in Section III the space step at higher frequencies must be smaller than $\lambda/20$ where $\lambda$ is the wavelength corresponding to the highest frequency of interest.

These two conditions imply that the mesh must be dense inside the structure and that the computational domain must be large. Since a uniform grid would not be computationally efficient for such problems we have used a nonuniform mesh. In order to avoid spurious reflections resulting from abrupt changes of space step, the node spacing is smoothly increased from slightly under $\lambda_1/20$ ($\lambda_1$ being the freespace wavelength of the highest frequency of interest) to a space step of $\lambda_2/10$ ($\lambda_2$ being the wavelength corresponding to the cutoff frequency).

To further reduce the required amount of memory by a factor of 2, it is possible to make use of the symmetry of the structure. The modes of the image guide are classified as $E^x_{mn}$ and $E^y_{mn}$ modes. Therefore, when $m$ is odd/even a perfect magnetic/electric wall is placed at $x = 0$, respectively.

### D. Data Analysis

Once the FDTD temporal response has been obtained using two probes located along the axis of propagation at a distance $z = L_1$ and $z = L_2$, the propagation constant $K_z$ is given by the Fourier transform of the responses of the two probes [4]. The losses are assumed negligible. In practice, several probes are located in the substrate at $x = a/2$, $y = b/2$ at various positions in the $z$ direction. A fast Fourier transform is performed on sets of two probes to calculate the propagation constant $K_z$. The pairs are chosen at random but it has been found that the distance between two probes of a same pair must be greater than one waveguide wavelength of the frequency of interest in order to achieve good accuracy. To avoid small variations in the results which arise from probe pairs at the extremes of a wide frequency range an average value is used.

### E. Excitation of the Structure

To limit the CPU time requirements, it is desirable to produce results over a given frequency range by a single run of the 3-D FDTD version. To correctly excite the image guide with a given mode over a given frequency band, we use a pulse at $z = 0$ having the field pattern of the desired mode at the center frequency of the band. To do this, we use the technique described in [13]:

The first step is similar to that proposed in [9], [10] in that a two-dimensional FDTD approach is used with a fixed value of the propagation constant $K_z$ and a short pulse (typically of time constant $T = 1$ ps) as the excitation. The transmission line to be analyzed is assumed to be uniform in the $z$ direction and have the properties of the specified geometry in the plane $z = 0$. In this paper, the FDTD is carried out in the cross section only, i.e., no portion of mesh is considered in the direction of propagation. After a fast Fourier transform, the frequencies in the Fourier spectrum correspond to the possible modes coinciding with the values of $K_z$. The first peak is the fundamental mode, the following ones are the higher order modes. Doing this corresponds to running a 2-D FDTD and we obtain the propagation characteristics at a particular frequency (the CPU time is a few minutes on a Hewlett Packard HP 720).

However, if we are interested in the characteristics over a wide frequency range then instead of performing a number of runs with various values of $K_z$, a quicker way to operate consists in taking a template of the mode and then using a three-dimensional FDTD method. Having ascertained the characteristic frequencies for the mode of interest we repeat the 2-D run but this time we calculate the sums

$$\sum_{n=1}^{N} E(n\delta t)\exp(j\omega_s n\delta t) \tag{12}$$

where

$$N = K_s \frac{2\pi}{\omega_s \delta t}$$

$K_s$ is an integer and $\omega_s$ is the angular frequency of interest.

These sums are accumulated as snapshots of the field pattern; Fig. 2 shows the result for the modes $E^y_{11}$ and $E^y_{31}$ of the image guide.

A three-dimensional FDTD method is then generated with the template snapshot at $z = 0$ together with a modulated Gaussian pulse as the excitation. The modulation frequency of the pulse is the same as that used to create the template and the time constant is chosen to cover the whole frequency range of interest. The 3-D results are identical to the 2-D results.

Note that coupling may in principle occur from one mode to another by utilizing this template technique. However, in the case of this type of image guide, little coupling will occur as the modes investigated have very distinct $K_z$ and field configuration, therefore the coupling overlap integral is very small.

It has been found that results for the low frequency characteristics of the structure are sensitive to the excitation field pattern and in order to get accurate results from dc up to high frequencies a good compromise consists of choosing an excitation template having a frequency content corresponding to a value of $K_z/K_0 \simeq 1.1$ in the dispersion diagram. For a more reduced frequency range however, the template can be taken at a frequency corresponding to the middle of the frequency range.

The CPU time for a 3-D run is 35 min on an HP720 to calculate the complete dispersion characteristic for any given mode of the image guide.

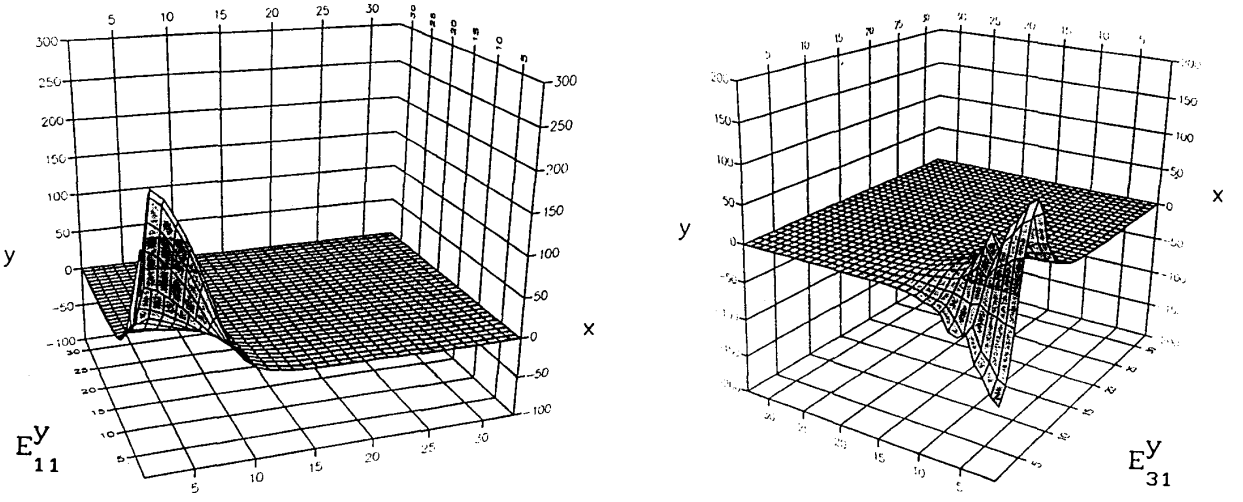


Fig. 2. Example of 2-D template snapshots used for excitation of the $E^y_{11}$ and $E^y_{31}$ modes of the image guide.

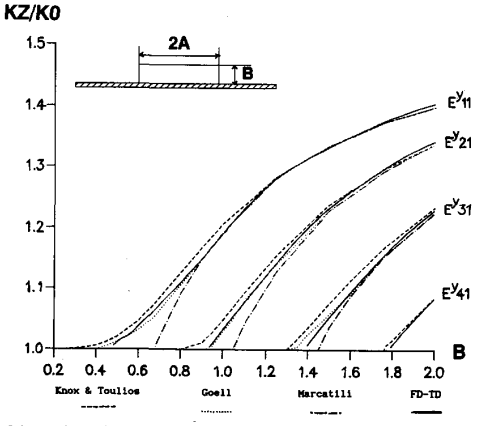


Fig. 3. Dispersion diagram of the first four modes of an image guide.

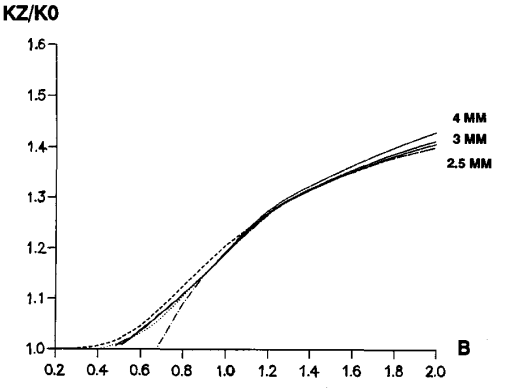


Fig. 4. Effect of the region sizes in the $z$ direction on the propagation characteristics of the fundamental mode of the image guide.

## III. Results

### A. Single Image Guide

Our technique has been tested on a low permittivity substrate image guide. In Fig. 3, $K_z/K_0$ is plotted against the normalized height $B = 4b\sqrt{\epsilon_r - 1}/\lambda_0$ for the first four modes of the image guide and comparison is made to results found in [1]. For small and moderate values of $B$ very good agreement is obtained between the FDTD technique and Goell's rigorous analysis [3].

For large values of $B$ a discrepancy arises when the energy is more closely confined into the dielectric. The FDTD region sizes (Table I) are fixed to 2.5 mm inside the dielectric and only give accurate results up to $B \simeq 2$ ($f$=25 GHz). Fig. 4 shows that the response predicted by the FDTD method is strongly conditioned by the region sizes in the direction of propagation. Hence, because of large memory requirements and long CPU times, accurate 3-D results using the FDTD method are difficult to achieve for large values of $B$. This is a minor drawback as in the most interesting part of the curve (monomodal behavior and determination of the cutoff frequencies of higher order modes), the FDTD technique provides good accuracy and higher order modes are as easily characterized as the fundamental one.

TABLE I
Region Sizes for the Single Image Guide ($a = 2b = 10$ mm, $\epsilon_r = 2.25$)

| direction | number of regions | regions sizes (in mm) |
|---|---|---|
| x | 11 | 5 x 2.5, 3, 3.5, 5, 7, 10, 15 |
| y | 6 | 3 x 2.5 , 5 , 8 , 15.5 |
| z | 50 | 50 x 2.5 |
| number of nodes | 211.200 (knodes) | (4 nodes per region) |

### B. Image Guide Coupler

Fig. 5 shows the dimensions of the $X$-band coupler and the region sizes are shown in Table II. The 2-D template was taken at $f = 9.5$ GHz and a perfect magnetic/electric wall

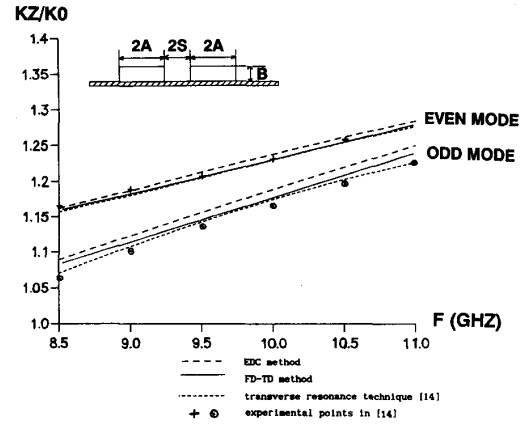


Fig. 5. Dispersion characteristics of an image guide coupler.

TABLE II
REGION SIZES FOR THE COUPLED IMAGE GUIDES
($a = 2b = 10$ mm, $s = 2.5$ mm, $\epsilon_r = 2.88$)

| direction | number of regions | regions sizes (in mm) |
|---|---|---|
| x | 14 | 2.5, 5 x 4, 4, 5, 6, 7, 8, 9, 10,15 |
| y | 7 | 2 x 2.5 , 3 , 4 , 5, 7, 10 |
| z | 32 | 32 x 5 |
| number of nodes | 200.704 (knodes) | (4 nodes per region) |

was used at $x = 0$ according to the mode under consideration (even/odd).

The 3-D FDTD result is shown in Fig. 5 where $K_z/K_0$ is plotted together with other theoretical and experimental results from [14] and results computed after [1]. The FDTD results agree very well with those obtained by the rigorous transverse resonance technique [14], especially for the even mode of the coupler. For both modes, FDTD results are closer to the experimental values than those obtained by the EDC method.

## IV. CONCLUSION

In this paper, dispersion characteristics of single and coupled open image guides of low permittivity have been investigated using an improved three-dimensional Finite-Difference Time-Domain technique and an accuracy comparable to that obtained by other rigorous techniques has been obtained for the fundamental mode as well as for higher order modes of the structure. Rigorous modeling of multidimensional dielectric boundaries and incorporation of a nonuniform mesh are achieved by modifying the standard FDTD equations and this allows a more versatile mesh to be implemented around dielectric boundaries. Due to the use of a nonregular mesh, a moderate number of nodes was used. Advantages of the FDTD method include its versatility and the fact that no pre-analytical treatment is required for different structures. The rigorous three-dimensional FDTD version has its own interest as it constitutes a first step to the characterization of discontinuities and hence to more complex structures.

## ACKNOWLEDGMENT

The authors would like to thank Prof. J. P. McGeehan for provision of facilities at the Centre for Communications Research and are grateful to GPT Ltd. and SERC U.K. for financial support.

## REFERENCES

[1] R. M. Knox and P. P. Toulios, "Integrated circuits for the millimeter through optical frequency range," in *Proc. Symp. Submillimeter Waves*, Pol. Inst. of Brooklyn, Mar. 31–Apr. 1–2, 1970, pp. 497–516.
[2] T. Itoh, *Dielectric Waveguide-Type Millimeter-Wave Integrated Circuits*. New York: Academic, 1981.
[3] J. E. Goell, "A circular-harmonic computer analysis of rectangular dielectric waveguides," *Bell Syst. Tech. J.*, vol. 48, pp. 2133–2160, Sept. 1969.
[4] X. Zhang, J. Fang, K. K. Mei, and Y. Liu, "Calculations of the dispersive characteristics of microstrips by the time-domain finite-difference method," *IEEE Trans. on Microwave Theory Tech.*, vol. 36, pp. 263–267, Feb. 1988.
[5] D. M. Sheen, S. M. Ali, M. D. Abouzahra, and J. A. Kong, "Application of the three-dimensional finite-difference time-domain method to the analysis of planar microstrip circuits," *IEEE Trans. Microwave Theory Tech.*, vol. 38, pp. 849–857, July 1990.
[6] D. L. Paul, E. M. Daniel, and C. J. Railton, "Fast finite difference time domain method for the analysis of planar microstrip circuits," in *Proc. 21st Europ. Microwave Conf.*, Stuttgart, Germany, 1991, pp. 303–308.
[7] S. T. Chu and S. K. Chaudhuri, "A finite-difference time-domain method for the design and analysis of guided-wave optical structures," *J. Lightwave Technol.*, vol. 7, pp. 2033–2038, Dec. 1989.
[8] W. K. Gwarek, "Application of time-domain methods to calculation of dispersion characteristics of transmission lines of arbitrary cross section," in *Proc. Numelec Conf.*, Grenoble, France, vol. 1, 1991, pp. 1–4.
[9] S. Xiao, R. Vahldieck, and H. Jin, "Full-wave analysis of guided wave structures using a novel 2-D fdtd," *IEEE Microwave Guided Wave Lett.*, vol. 2, pp. 165–167, May 1992.
[10] V. J. Brankovic, D. V. Krupezevic, and F. Arndt, "An efficient two-dimensional graded mesh finite-difference time-domain algorithm for shielded or open waveguide structures," *IEEE Trans. Microwave Theory Tech.*, vol. 40, pp. 2272–2277, Dec. 1992.
[11] C. J. Railton and J. P. McGeehan, "An analysis of microstrip with rectangular and trapezoidal conductor cross sections," *IEEE Trans. Microwave Theory Tech.*, vol. 38, pp. 1017–1022, Aug. 1990.
[12] G. Mur, "Absorbing boundary conditions for the finite-difference approximation of the time-domain electromagnetic-field equations," *IEEE Trans. Electromagn. Compat.*, vol. 23, pp. 377–382, Nov. 1981.
[13] C. J. Railton and J. P. McGeehan, "The use of mode templates to improve the accuracy of the finite-difference time-domain method," in *Proc. 21st Europ. Microwave Conf.*, Stuttgart, Germany, 1991.
[14] S. Toutain, "Contribution à l'étude du guide image: Mise en évidence d'ondes à fuites," Ph.D. dissertation, Univ. of Lille, 1986. Thèse de Doctorat d'Etat.

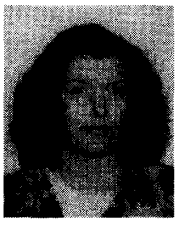

**Dominique-Lynda Paul** was born in Blida, Algeria, on January 16, 1961. She received the D.E.A. degree in electronics from Brest University in June 1986 and the Ph.D. degree from the "Ecole Nationale Supérieure des Télécommunications de Bretagne" (LEST-ENSTBr) in January 1990.

She is now working as a post-doctoral research associate at the Communications Research Centre, University of Bristol. Her research interests include the modeling of passive planar microstrip devices and the characterization of dielectric systems at millimeter wavelengths.

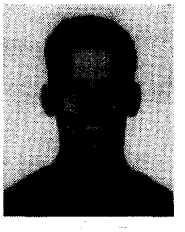

**Nick M. Pothecary** received the B.Eng. (Hons) degree in electrical and electronic engineering from the University of Bristol in 1990.

He is now working towards the Ph.D. at the Centre for Communications Research, University of Bristol. His research interests include the numerical modeling of electromagnetic waves for communication, industrial, and medical applications. He has also spent some time at the Ecole Nationale Supérieure des Télécommunications de Bretagne, working on speech coding techniques.

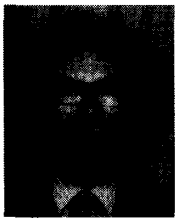

**Chris J. Railton** received the B.Sc. degree in physics with electronics from the University of London in 1974 and the Ph.D. degree in electronic engineering from the University of Bath in 1988.

During the period 1974–1984 he worked in the scientific civil service on a number of research and development projects in the areas of communications and signal processing. Between 1984 and 1987 he worked at the University of Bath on the mathematical modeling of boxed microstrip circuits. He currently works in the Centre for Communications Research at the University of Bristol where he leads a group involved in the mathematical modeling and development of CAD tools for MMICs, planar antennas, microwave heating systems, EMC, and high speed logic.